Elevated Electron Temperature Coincident with Observed Fusion Reactions in a Sheared-Flow-Stabilized Z Pinch

B. Levitt,[1,*] C. Goyon,[2] J. T. Banasek,[3] S. C. Bott-Suzuki,[3] C. Liekhus-Schmaltz,[1] E. T. Meier,[1] L. A. Morton,[1] A. Taylor,[1] W. C. Young,[1] B. A. Nelson,[1] D. A. Sutherland,[1] M. Quinley,[1] A. D. Stepanov,[1] J. R. Barhydt,[1] P. Tsai,[1] K. D. Morgan,[1] N. van Rossum,[1] A. C. Hossack,[1] T. R. Weber,[1] W. A. McGehee,[1] P. Nguyen,[1] A. Shah,[1] S. Kiddy,[1] M. Van Patten,[1] A. E. Youmans,[2] D. P. Higginson,[2] H. S. McLean,[2] G. A. Wurden,[4] and U. Shumlak[1,5,†]

[1]*Zap Energy Inc., Seattle, Washington 98203, USA*

[2]*Lawrence Livermore National Laboratory, 7000 East Avenue, Livermore, California 94550, USA*

[3]*University of California San Diego, La Jolla, California 92093, USA*

[4]*Los Alamos National Laboratory, Los Alamos, New Mexico 87545, USA*

[5]*Aerospace and Energetics Research Program, University of Washington, Seattle, Washington 98195, USA*

(Received 27 January 2023; revised 28 April 2023; accepted 31 January 2024; published 8 April 2024)

The sheared-flow-stabilized Z pinch concept has been studied extensively and is able to produce fusion-relevant plasma parameters along with neutron production over several microseconds. We present here elevated electron temperature results spatially and temporally coincident with the plasma neutron source. An optical Thomson scattering apparatus designed for the FuZE device measures temperatures in the range of 1–3 keV on the axis of the device, 20 cm downstream of the nose cone. The 17-fiber system measures the radial profiles of the electron temperature. Scanning the laser time with respect to the neutron pulse time over a series of discharges allows the reconstruction of the T_e temporal response, confirming that the electron temperature peaks simultaneously with the neutron output, as well as the pinch current and inductive voltage generated within the plasma. Comparison to spectroscopic ion temperature measurements suggests a plasma in thermal equilibrium. The elevated T_e confirms the presence of a plasma assembled on axis, and indicates limited radiative losses, demonstrating a basis for scaling this device toward net gain fusion conditions.

DOI: 10.1103/PhysRevLett.132.155101

Since fusion reactivity depends sensitively on plasma temperature [1], accurate temperature measurements are critically important. Historically, determination of electron temperature using Thomson scattering has been a reliable technique to validate plasma temperature [2] and its correspondence with other measurements [3]. In cases of plasma thermal equilibrium, electron temperature T_e is a valid indicator of bulk plasma temperature, and therefore ion temperature T_i, upon which fusion reactivity depends. As such, T_e can be used in these cases to understand and predict fusion performance [4].

Electron temperature in high temperature fusion-relevant plasmas is often considered a qualitative measure of plasma *health*, in the sense that various loss mechanisms are manifested in the electron channel. Electron energy loss mechanisms include line radiation in plasmas with high impurity content [4] and electron axial losses [5]. In adiabatically compressed plasmas such as those studied in this Letter [6–8], typically $T_e < T_i$. Electron-ion collisions cool ions at a rate that is proportional to $T_e^{-3/2}$. Thus, elevated electron temperature, comparable to ion temperatures, suggests good electron confinement and precludes detrimental cooling of ions by electrons via these mechanisms.

The well known instabilities which have historically prevented high performance fusion operation in Z pinches [5,9–11] have been shown computationally and experimentally to be stabilized by the application of radially sheared axial plasma flows [6,12–15]. Scaling of these sheared-flow-stabilized (SFS) Z pinches toward net gain fusion energy production shows promise, and would constitute an extremely compact, simple, and economical commercial fusion device [16–18].

Here, we present the first spatially and temporally localized equilibrium T_e measurements from the core of the SFS Z-pinch plasma in the keV range. These measurements confirm earlier indications of both T_e and T_i (from nonlocalized chord-integrated measurements [6,7] which could be sensitive to turbulent or other broadening effects) and suggest thermal equilibration between ions and electrons in the deuterium plasma. Similar to recent work [4], we observe $T_e \leq T_i$. As such, establishing T_e as a lower bound for T_i sets a lower limit for fusion rate predictions. Here, the associated heating mechanism is predicted to be adiabatic compression, which heats both ions and electrons [8].

Plasma parameters and fusion performance of the SFS Z pinch have been measured using a variety of diagnostic

techniques [6–8,19–21]. T_i has been determined spectroscopically from Doppler broadening of impurity emission lines [7,21]. The sum of electron and ion temperatures [6] has been measured by combining density profiles extracted from digital holographic interferometry [19] and magnetic field probes [13] and assuming equilibrium radial force balance in the Z-pinch plasma. The electron temperature has been directly measured using Thomson scattering on the ZaP SFS Z-pinch device, when operating at low plasma performance, to show $T_e = 64$ eV [7]. Spectroscopic measurements indicated $T_i = 71$ eV, and force balance resulted in $T_e + T_i = 160$ eV, in qualitative agreement to the experimental total of 135 eV, suggesting that the computed equilibrium values are valid.

The Thomson scattering (TS) system, along with its initial results on FuZE, has been discussed previously [22]. In Ref. [22], the details of the diagnostic subsystems and the methodologies for inferring the values of T_e are presented. The results presented in Ref. [22] featured unoptimized pulses on the FuZE device, with T_e measurements in the range of 300–700 eV. By contrast, the data presented in this Letter analyze Thomson features generated from optimized FuZE performance and correlates them to contemporaneous neutron production rates. Here, we report peak electron temperatures in the range of 1–3 keV, temporally coincident with high neutron production rates.

The FuZE device generates a sheared-flow-stabilized Z-pinch plasma which, depending on the pulsed driver current waveform and details of the fast gas injection, can last from 1–10 μs. The lifetime is limited by these engineering constraints, not the growth rates of the typical magnetohydrodynamics modes observed in Z-pinch devices. Indeed, the FuZE discharge endures for 1000 to 10 000 growth times of the $m = 0$ and $m = 1$ modes [8,21,23]. Typical axial extents of the pinches also range, depending on the above parameters, from several centimeters up to the length of the *assembly* region in the device, extending 50 cm from the upstream nose cone to the downstream end wall (see details of Fig. 1). Pure deuterium discharges are accompanied by the generation of thermonuclear fusion reactions within the pinch [24]. The associated 2.45 MeV neutrons are detected by a spatial array of fast plastic scintillators (S) coupled to photomultiplier tubes (PMT). (The short hand of SPMT will be used to refer to these detectors.) These measurements were consistent with a thermal fusion [24] linear neutron source [20] that is approximately 32 cm long.

For the data set analyzed in this Letter, the neutron source has increased significantly since the above referenced publications. Average neutron production rates achieved in current FuZE operation are $\approx 3 \times 10^7$ n/μs, up from $\approx 6 \times 10^5$ n/μs [21]. Typical plasma measurements indicate T_i in the range of 1–3 keV, as measured by Doppler broadening of impurity carbon, densities of approximately 10^{17} cm^{-3}, and pinch radii in the range of 3–10 mm. Differences in plasma performance between this and previous works are due to the usage of a different pulsed-power current driver.

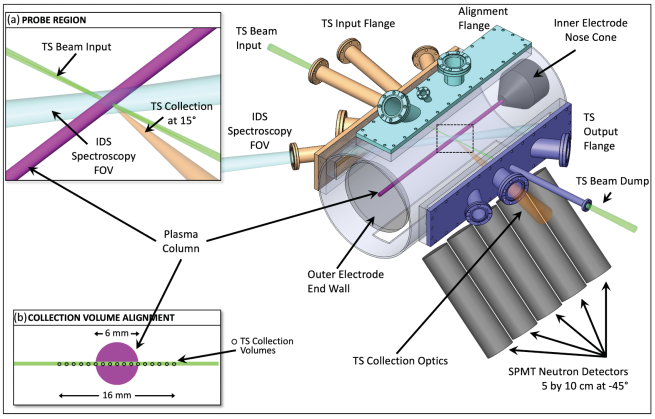

FIG. 1. The Z-pinch assembly region of the FuZE device and TS system, featuring three dedicated vacuum flanges for the TS system. The assembly region of the device extends from the upstream nose cone down to the end wall. Also shown are views of the UV spectroscopy measurement for T_i as well as placement of the axial SPMT array, at bottom right. (a) Detail of the probe region and collection region, which is indicated by the dashed square in the main figure; (b) end-on view of the idealized plasma column and radial extent of the TS collection volumes. Vertical displacements of the plasma column results in TS collection volumes that do not coincide with the Z-pinch plasma axis.

The TS system, shown in Fig. 1, focuses an 8 J, 1.4 ns, 532 nm probe laser 20 cm downstream from the nose cone. The Thomson scattered signal from the probe beam is collected at a 150° angle via an optical doublet and linear fiber array each of 100 μm diameter. The output of the fiber is coupled to a spectrometer and time-gated camera assembly to resolve the scattered spectrum. The TS system probes the plasma at 17 locations along the laser beam path for a 1.6 cm total field of view, each probed volume being ≈ 0.5 mm^3.

Examples of observed responses from two FuZE discharges are shown in Fig. 2. The raw spectra are shown in the left panels, each collected from a different radial location at the same axial location. Three fibers are shown for each pulse, representing three radial locations. We used a 4 ns camera-integration time and a notch filter to reject the signal around the laser wavelength and avoid saturating the detector with "stray light." To infer T_e, a spectrum is fitted by a noncollisional Thomson scattering model using three free parameters; T_e, the signal peak intensity, and the continuum intensity. Each fit is represented by a blue line in the right panels. (The reconstructed T_e radial profile using each fiber location is shown below in Fig. 4).

TS spectra collected at this axial location on FuZE suggest n_e lower than 5×10^{16} cm^{-3}, which is beyond the resolution of the diagnostic. Therefore, we used two fixed values of 5×10^{15} cm^{-3} and 5×10^{16} cm^{-3} to calculate the

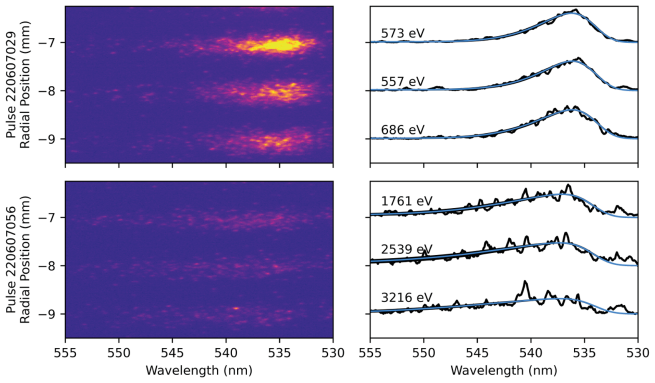

FIG. 2. Raw Thomson data (left column) and fits (right column) for three representative fibers from two FuZE pulses: pulse 220607029 on the top row and pulse 220607056 on the bottom row. The fitted T_e values are displayed in the right column for each chord. Increased broadening of the spectra represent higher plasma temperatures. The reconstruction of the full radial profiles are shown below in Fig. 4.

error bar on T_e [22]. For n_e lower than 5×10^{15} cm^{-3} the measurement is fully noncollective, and the width of the spectrum is no longer influenced by n_e, and does not affect the inferred T_e.

The reported T_e values assume a single Maxwellian electron population. Although a portion of the spectrum is blocked by the notch filter, our fits can still accurately infer temperatures down to 100 eV. As such, these measurements strongly limit possible deviations from Maxwellian. Such effects would lead to only small changes in T_e and are therefore captured in our error bars.

Still, mechanisms that generate non-Maxwellian behavior can be considered. For example, if an instability-driven electron beam were present [9] it would propagate *away* from the FuZE inner electrode (cathode), causing blueshifts. Such bulk blueshifts would in fact lead to the analysis in this Letter *underestimating* the electron temperature. Beyond these fundamental difficulties, there is no observable from this data set or the large body of experimental work on SFS Z pinches to motivate such a strong non-Maxwellian contribution. Thus, the assumption of a single Maxwellian population is well supported, and small deviations from this are captured in the error bars.

Pulse 220607029 in the top row of Fig. 2 is consistent with peak T_e fits of 1.5 keV, while pulse 220607056 in the bottom row is broadened substantially more, giving peak fits of 3.2 keV. For $T_e \approx 1$ keV, we note that the thresholds for plasma heating by inverse bremsstrahlung are approximately 3 orders of magnitude above the measured densities; therefore these processes do not influence the inferred T_e.

The plot in Fig. 3(a) shows a typical FuZE discharge during this campaign; qualitatively similar figures have been published and described in detail for FuZE operation [21]. Total plasma current across the anode and cathode gap is

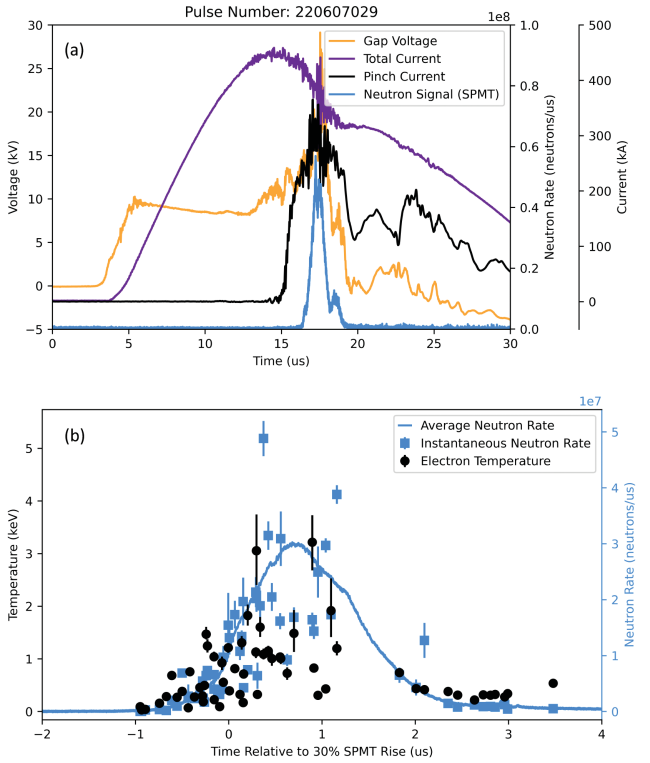

FIG. 3. (a) A typical FuZE pulse taken during this campaign. The total plasma current in the accelerator is measured at the upstream anode-cathode gap [8] and is plotted in purple; the current that makes it into the pinch is black; the voltage drop across the anode-cathode, V_{gap}, is orange; and the neutron production rate as measured by a SPMT detector is blue. The peak in V_{gap} is coincident with the peak in pinch current as well as the onset of neutron production. (b) Reconstruction of the temporal evolution of the electron temperature over many pulses on the same timescale as the neutron production rate. (The TS delay is reported with respect to the rise time of the SPMT signal, defined as 30% of peak signal.) The solid blue line is averaged over all of the relevant pulses. The blue dots are the instantaneous neutron production rate for each pulse, integrating over a 200 ns window. We observe temporal coincidence of T_e and the neutron production rate.

measured at the upstream breach of the accelerator [8] and is plotted in purple; pinch current measured in the assembly region where the pinch forms and compresses is plotted in black; the voltage measured at the accelerator breach V_{gap} is given in orange; and the neutron production rate measured by an SPMT operating in analog mode is plotted in blue. As noted in previous work, the peak in neutron production is coincident with the peak in the pinch current as well as a large inductive increase in the V_{gap} signal, which is understood to be generated from pinch formation and compression.

To investigate the temporal correlation of neutron production with T_e, a series of pulses were taken where the Thomson probe laser delay was sequentially increased through the FuZE pulse. For each pulse, the TS delay is

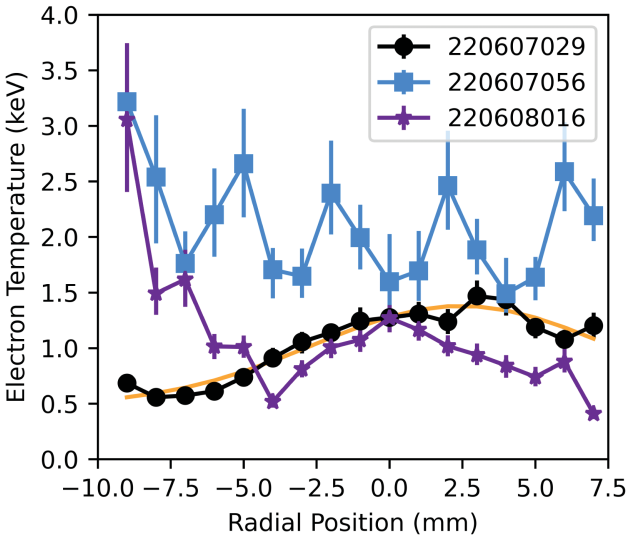

FIG. 4. Three representative pulses showing examples of the T_e spatial extents observed in the TS campaign. Large pulse-to-pulse variation is seen, from a radially localized on-axis response (black trace) to a broad flat response across all channels (blue trace). A Gaussian FWHM fit to pulse 220607029 (orange trace) gives a ≈6 mm pinch radius.

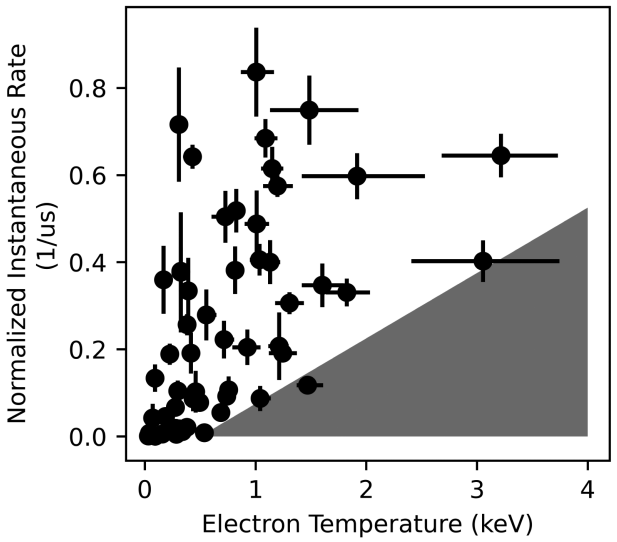

FIG. 5. Plot of the normalized instantaneous neutron production rate versus the T_e measurements. The values for rate are calculated by integrating a 200 ns window of the SPMT signal centered around the Thomson laser trigger. The triangle at bottom right indicates the region of parameter space characterized by low neutron production and high T_e, which is not observed experimentally.

reported with respect to the rise time of the SPMT detector signal, defined as 30% of peak signal. This delay has been quantified to within 5 ns and corrects for the jitter in bank firing, ≈1 μs. Figure 3(b) plots T_e against the neutron production rate for 59 identically prepared pulses. The black dots show the maximum T_e across the TS field of view and the blue dots indicate the instantaneous neutron production rate. The latter is computed by integrating the analog SPMT response over a 200 ns window centered around the TS laser trigger. The neutron production rate averaged over all of the relevant pulses is shown as a solid blue line.

We observe in Fig. 3(b) that T_e rises above 1 keV as the neutron production rate increases, and comes down below 1 keV as the neutron production rate declines at ≈2 μs. At the peak of the neutron production rate, 0–1 μs, T_e reaches its highest values up to 3 keV. This qualitative agreement suggests the temporal rise, peak, and subsequent fall of T_e are synchronized with those of the neutron production rate and pinch current.

Though these pulses were prepared identically, we observe variation in the derived T_e data. For example, in Fig. 3(b) near 1 μs one observes several pulses ranging from ≈400 eV to ≈3 keV. We considered two possible explanations for these variations. The first is the motion of the plasma column: the core of the pinch can be displaced from the TS collection volume [23] leading to lower observed T_e. A second explanation is pulse-to-pulse differences in plasma performance, which could lead to variations in plasma structure.

An appreciation of the variation observed by the Thomson system is illustrated in Fig. 4, which shows T_e across all observation points for three pulses (two of which are the same pulses presented in Fig. 2). Pulse 220607029 indicates a spatially localized on-axis structure with a radius of ≈6 mm; pulse 220608016 measures significantly higher temperature displaced off-axis by 1 cm on the leftmost chord, which nearly misses the TS collection volume entirely; and pulse 220607056 shows an even hotter but much broader distribution. The radial structure seen in the profiles provides peak temperatures to characterize the plasma properties instead of relying on the average temperature. The pulse-to-pulse variance underlies the scatter in the temporal data in Fig. 3, and is also observed in other spectroscopic measurements on FuZE.

Figure 5 replots the data from Fig. 3(b) between the peak magnitudes of T_e with the instantaneous SPMT neutron production rate. Given the spread in both T_e and neutron rate measurements, the main feature is that elevated T_e and high neutron production rate are typically coincident, while lower T_e appears uncorrelated with neutron production. This results in the triangular distribution seen in the plot, since there are no observations of low neutron production rate and high temperature. The lack of these observations is emphasized by the gray region at bottom right. This feature is consistent with the explanation that the low-T_e/high-production rate data points are due to a plasma column displaced from the TS collection volume. Thermal fusion yield is also driven by plasma density and plasma volume, which are not measurements discussed here. Thus, elevated T_e gives a necessary but not sufficient condition for elevated yield, which may further explain the observations.

The limitations of the correlation are the result of the comparison of a spatially global and time-integrated measurement with a both spatially and temporally localized measurement. Further substantiation ideally requires T_e measurements at all locations and times within the device. Future expansions of the spatial and temporal measurements will make some progress toward this end.

For an identically prepared series of plasma pulses, ion temperature was determined using ion Doppler spectroscopy (IDS) of carbon. Broadening of carbon-V triplet lines (227.1, 227.2, and 227.8 nm) were measured as a function of time during the FuZE pulse, comparable to the TS data in Fig. 3. The IDS spectrometer requires a longer collection gate of 1.0 μs, resulting in less temporal resolution. As such, we quote a value of peak T_i across all IDS chords, averaged over 24 pulses which were acquired within 0 to 1.5 μs of the neutron emission period: $T_i = 1.4 \pm 0.5$ keV. This can be compared to the average T_e during this same time window: $T_e = 1.1 \pm 0.8$ keV. Thus, within error these measurements give an indication of thermal equilibration between ions and electrons. However, for these conditions carbon is fully stripped after only 1 μs [25], such that carbon-V is likely burnt out of the core pinch, existing primarily in the cooler periphery. Thus, a more conservative conclusion would be that $T_e \leq T_i$, since the maximum T_i in the plasma may be more elevated than the IDS carbon-V analysis can reliably measure.

In typical Z-pinch plasmas, hot ions collisionally couple and heat electrons via thermal equilibration, while electron energy is subsequently lost through radiation and other mechanisms. Recent observations [4] corroborate this scenario, showing $T_e \leq T_i$, consistent with the FuZE measurements discussed here. Thus, T_e provides a lower bound for T_i, and the associated thermonuclear fusion reactivity. Reference [4] also discusses ion Doppler-inferred temperature as a *pseudotemperature* that can be higher than actual thermal T_i due to contributions from turbulent motion. The lower bound given by T_e limits this turbulent contribution.

The TS system measurement, resulting from a direct interrogation of the bulk deuterium plasma, provides the most reliable measure of temperature of the pinch core on the FuZE device. Since fusion reactivity is dependent on T_i and not T_e, the indication that the local measurement of T_e is a lower bound for T_i provides a solid basis for calculating fusion rates. The thermal fusion neutron yield from a pure deuterium Z-pinch plasma [21] for ≈1.5 keV and 5×10^{16} cm^{-3} and a plasma volume characterized by a 6 mm radius and 30 cm long 250 kA pinch gives a production rate of $\approx 4 \times 10^7$ n/μs. This estimate is in excellent agreement with the measured peak rates shown in Fig. 3. Whole device modeling of FuZE using the WARPXM code [26] and MACH2 code [8] closely reproduce observations, including T_i and T_e in the 1–3 keV range, as well as thermonuclear fusion yields in the 10^7 to 10^8 range.

The measurements presented here are the first direct confirmations of a keV regime equilibrium plasma temperature in the core of the SFS Z pinch. Observations made on these devices are consistent with ion-electron thermal equilibration, from the 100 eV level [6,7] up to current operations on FuZE, in the range of 1–3 keV. Further, the demonstration of elevated electron temperature puts a limit on thermal losses both from radiation enhanced by plasma impurities as well as excessive axial transport. These results are consistent with earlier measurements which suggest an adiabatically compressed [18] and stabilized pinch in radial force balance equilibrium [6,7] producing thermonuclear fusion [24]. This Letter supports continued efforts to scale the SFS Z pinch concept toward higher performance.

The information, data, or work presented herein was funded in part by the Advanced Research Projects Agency-Energy (ARPA-E), U.S. Department of Energy, under Awards No. DE-AR0001165, No. DE-AR-0000571, No. DE-AR-0001010, and No. DE-AR-0001260 and prepared by LLNL under Contract No. DE-AC52-07NA27344.

The views and opinions of authors expressed herein do not necessarily state or reflect those of the United States Government or any agency thereof.

*blevitt@zap.energy
†shumlak@uw.edu

[1] H. S. Bosch and G. M. Hale, Improved formulas for fusion cross-sections and thermal reactivities, Nucl. Fusion **32**, 611 (1992).
[2] N. J. Peacock, D. C. Robinson, M. J. Forrest, P. D. Wilcock, and V. V. Sannikov, Measurement of the electron temperature by Thomson scattering in Tokamak t3, Nature (London) **224**, 488 (1969).
[3] A. M. Anashin, E. P. Gorbunov, D. P. Ivanov, S. E. Lysenko, N. J. Peacock, D. C. Robinson, V. V. Sannikov, and V. S. Strelkov, Experiments on laser and microwave probing of plasma, and measurements of the diamagnetic effect on the Tokamak T-3a installation, Sov. Phys. JETP **33**, 1127 (1971).
[4] Y. Maron, Experimental determination of the thermal, turbulent, and rotational ion motion and magnetic field profiles in imploding plasmas, Phys. Plasmas **27**, 060901 (2020).
[5] M. G. Haines, A review of the dense Z-pinch, Plasma Phys. Controlled Fusion **53**, 093001 (2011).
[6] U. Shumlak, B. A. Nelson, E. L. Claveau, E. G. Forbes, R. P. Golingo, M. C. Hughes, R. J. Oberto, M. P. Ross, and T. R. Weber, Increasing plasma parameters using sheared flow stabilization of a Z-pinch, Phys. Plasmas **24**, 055702 (2017).
[7] U. Shumlak, C. S. Adams, J. M. Blakely, B.-J. Chan, R. P. Golingo, S. D. Knecht, B. A. Nelson, R. J. Oberto, M. R. Sybouts, and G. V. Vogman, Equilibrium, flow shear and stability measurements in the Z pinch, Nucl. Fusion **49**, 075039 (2009).

[8] U. Shumlak, *Z*-pinch fusion, J. Appl. Phys. **127**, 200901 (2020).
[9] Oscar A. Anderson, William R. Baker, Stirling A. Colgate, John Ise, and Robert V. Pyle, Neutron production in linear deuterium pinches, Phys. Rev. **110**, 1375 (1958).
[10] I. V. Kurchatov, On the possibility of producing thermonuclear reactions in a gas discharge, J. Nucl. Energy **4**, 193 (1957).
[11] A. L. Velikovich, R. W. Clark, J. Davis, Y. K. Chong, C. Deeney, C. A. Coverdale, C. L. Ruiz, G. W. Cooper, A. J. Nelson, J. Franklin, and L. I. Rudakov, *Z*-pinch plasma neutron sources, Phys. Plasmas **14**, 022701 (2007).
[12] U. Shumlak and C. W. Hartman, Sheared flow stabilization of the $m = 1$ kink mode in *Z* pinches, Phys. Rev. Lett. **75**, 3285 (1995).
[13] U. Shumlak, R. P. Golingo, B. A. Nelson, and D. J. Den Hartog, Evidence of stabilization in the *Z* pinch, Phys. Rev. Lett. **87**, 205005 (2001).
[14] U. Shumlak, B. A. Nelson, R. P. Golingo, S. L. Jackson, E. A. Crawford, and D. J. Den Hartog, Sheared flow stabilization experiments in the ZaP flow Z pinch, Phys. Plasmas **10**, 1683 (2003).
[15] U. Shumlak, J. Chadney, R. P. Golingo, D. J. Den Hartog, M. C. Hughes, S. D. Knecht, W. Lowrie, V. S. Lukin, B. A. Nelson, R. J. Oberto, J. L. Rohrbach, M. P. Ross, and G. V. Vogman, The sheared-flow stabilized *Z*-pinch, Fusion Sci. Technol. **61**, 119 (2012).
[16] E. G. Forbes, U. Shumlak, H. S. McLean, B. A. Nelson, E. L. Claveau, R. P. Golingo, D. P. Higginson, J. M. Mitrani, A. D. Stepanov, K. K. Tummel, T. R. Weber, and Y. Zhang, Progress toward a compact fusion reactor using the sheared-flow-stabilized *Z*-pinch, Fusion Sci. Technol. **75**, 599 (2019).
[17] M. C. Thompson, B. Levitt, B. A. Nelson, and U. Shumlak, Engineering paradigms for sheared-flow-stabilized *Z*-pinch fusion energy, Fusion Sci. Technol. **79**, 1051 (2023).
[18] B. Levitt, E. T. Meier, R. Umstattd, D. A. Sutherland, C. Liekhus-Schmaltz, B. A. Nelson, J. R. Barhydt, and I. A. M. Datta, The Zap Energy approach to commercial fusion, Phys. Plasmas **30**, 9 (2023).
[19] M. P. Ross and U. Shumlak, Digital holographic interferometry employing Fresnel transform reconstruction for the study of flow shear stabilized *Z*-pinch plasmas, Rev. Sci. Instrum. **87**, 103502 (2016).
[20] James M. Mitrani, Drew P. Higginson, Zack T. Draper, Jonathan Morrell, Lee A. Bernstein, Elliot L. Claveau, Christopher M. Cooper, Eleanor G. Forbes, Ray P. Golingo, Brian A. Nelson, Andrea E. Schmidt, Anton D. Stepanov, Tobin R. Weber, Yue Zhang, Harry S. McLean, and Uri Shumlak, Measurements of temporally- and spatially resolved neutron production in a sheared-flow stabilized *Z*-pinch, Nucl. Instrum. Methods Phys. Res., Sect. A **947**, 162764 (2019).
[21] Y. Zhang, U. Shumlak, B. A. Nelson, R. P. Golingo, T. R. Weber, A. D. Stepanov, E. L. Claveau, E. G. Forbes, Z. T. Draper, J. M. Mitrani, H. S. McLean, K. K. Tummel, D. P. Higginson, and C. M. Cooper, Sustained neutron production from a sheared-flow stabilized *Z* pinch, Phys. Rev. Lett. **122**, 135001 (2019).
[22] J. T. Banasek, C. Goyon, S. C. Bott-Suzuki, G. F. Swadling, M. Quinley, B. Levitt, B. A. Nelson, U. Shumlak, and H. S. McLean, Probing local electron temperature and density inside a sheared flow stabilized *Z*-pinch using portable optical Thomson scattering, Rev. Sci. Instrum. **94**, 023508 (2023).
[23] A. D. Stepanov, U. Shumlak, H. S. McLean, B. A. Nelson, E. L. Claveau, E. G. Forbes, T. R. Weber, and Y. Zhang, Flow z-pinch plasma production on the fuze experiment, Phys. Plasmas **27**, 112503 (2020).
[24] James M. Mitrani, Joshua A. Brown, Bethany L. Goldblum, Thibault A. Laplace, Elliot L. Claveau, Zack T. Draper, Eleanor G. Forbes, Ray P. Golingo, Harry S. McLean, Brian A. Nelson, Uri Shumlak, Anton Stepanov, Tobin R. Weber, Yue Zhang, and Drew P. Higginson, Thermonuclear neutron emission from a sheared-flow stabilized *z*-pinch, Phys. Plasmas **28**, 112509 (2021).
[25] P. G. Carolan and V. A. Piotrowicz, The behaviour of impurities out of coronal equilibrium, Plasma Phys. **25**, 1065 (1983).
[26] U. Shumlak, R. Lilly, N. Reddell, E. Sousa, and B. Srinivasan, Advanced physics calculations using a multi-fluid plasma model, Comput. Phys. Commun. **182**, 1767 (2011).